

in terms of vector bilocals with a gluon phase. The particular $\int dx$ moment considered is just such as to isolate the term linear in B in addition to the usual B -independent term.

¹⁷D. Broadhurst, J. F. Gunion, R. L. Jaffe, this issue, Phys. Rev. D **8**, 5661 (1973). Jackiw and Schnitzer (Ref. 5) have derived the spin- $\frac{1}{2}$ sum rule in a vector-gluon model but without the Regge subtraction terms inevitably present.

¹⁸An alternate derivation can be given by examining directly a sample interaction term.

¹⁹See F. E. Close and J. F. Gunion, Phys. Rev. D **4**, 742 (1971); V. R. Rittenberg and H. Rubinstein, Phys. Lett. **35B**, 50 (1971); E. D. Bloom and F. J. Gilman, Phys. Rev. Lett. **25**, 1140 (1970).

²⁰S. Coleman and S. Glashow, Phys. Rev. **134B**, 671 (1964); they give results for the elastic contributions. D. J. Gross and H. Pagels, Phys. Rev. **172**, 1381 (1968), also give a useful summary of the elastic contributions calculated using various assumptions. S. Coleman and H. J. Schnitzer, Phys. Rev. **136**, B223 (1964), obtain still different values using different assumptions.

²¹M. Damashek and F. J. Gilman, Phys. Rev. D **1**, 1319 (1970); C. A. Dominguez, C. Ferro Fontan, and R. Suaya, Phys. Lett. **31B**, 365 (1971).

²²C. A. Dominguez, J. F. Gunion, and R. Suaya, Phys. Rev. D **6**, 1404 (1972).

²³In fact, in a number of simple models incorporating both a strong and an electromagnetic substructure $(\delta m_\phi - \delta m_\pi) < 0$ to first order in α . I thank Ken Johnson for pointing this out.

²⁴M. Gell-Mann, R. J. Oakes, and B. Renner, Phys. Rev. **175**, 2195 (1968); S. Glashow and S. Weinberg, Phys. Rev. Lett. **20**, 224 (1968); R. A. Brandt and G. Preparata, Ann. Phys. (N.Y.) **61**, 119 (1970).

²⁵This was not necessary for the nucleons themselves due to the substantial size of \bar{M} in

$$M^2 - \bar{M}^2 = 2\bar{M}\delta M + (\delta M)^2.$$

The $(\delta M)^2$ term is down by a factor of 10 in all cases.

²⁶H. Alvensleben *et al.*, DESY report (unpublished).

²⁷This point is due to Ken Johnson.

²⁸S. Weinberg, private communication.

²⁹See the papers of Gunion, Brodsky, and Blankenbecler, Ref. 3.

Nonleading Regge Poles in Unitary Multiperipheral Models*

Steven P. Auerbach

Department of Physics, University of California, Berkeley, California 94720

(Received 2 March 1973)

Unitary multiperipheral models with two input trajectories are presented. It is shown that the nonleading output trajectories play a crucial role in determining the high-energy behavior of such models.

I. INTRODUCTION

All simple multiperipheral models share the problem that increasing the strength of the particle production mechanism eventually violates the Froissart bound. In a recent paper¹ (hereafter called I), a class of models was introduced which dealt with this difficulty by explicitly incorporating s -channel multiparticle unitarity. These models are specified by defining the amplitude W_n for two particles ("protons") to emit or absorb n particles ("pions") from a single chain which is exchanged between the two protons. If the links in the chain are Reggeons, the model described in I is a unitarized multi-Regge model.

A general feature of such models is that the checkerboard diagrams (Fig. 1) (where particles are emitted from any chain and absorbed by any other) give rise to a new type of cut in the angular momentum plane. This unitarity cut enforces the Froissart bound by cleverly arranging that any poles to the right of one are on an unphysical sheet

and thus do not contribute to the scattering amplitude.

Although the details of the cut are fairly complicated and model-dependent, the existence of such a cut can be traced to the simple fact that pairwise interaction between N chains, as shown in Fig. 1, leads to an output Regge pole whose position is proportional to $\frac{1}{2}N(N-1)$, the number of pairs of chains. Thus the sum over any number of chains will be a formally divergent series; this divergence, as shown in I, leads to the unitarity cut. Any multiperipheral model with pairwise interactions which does not expressly forbid multichain exchange will therefore have such a cut.

One defect of the models presented in I is their neglect of all low-subenergy effects. Sugar² has recently studied unitary models which include the effects of producing pairs of particles with low subenergies at any point along the chain. In this paper an attempt will be made to include low-subenergy effects along the lines laid down by Chew and Pignotti³ (hereafter called CP), who invoke

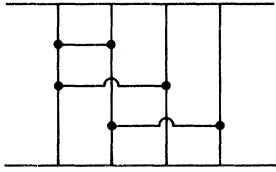


FIG. 1. A checkerboard diagram.

duality to argue that these effects will be approximately simulated by including lower-lying meson trajectories in addition to the Pomeranchuk trajectory. Following CP, only two trajectories will be included: A higher trajectory α_P (the Pomeranchuk trajectory) and a lower effective meson trajectory α_M .

The introduction of lower-lying trajectories, not surprisingly, leads to nonleading output Regge trajectories in addition to the leading trajectory. However, essentially the same counting argument as before shows that the nonleading output pole positions also grow with N as N^2 . Thus, there are divergences associated with the nonleading poles as well, which could well qualitatively change the conclusions of I.

There are two cases which are simple enough to be solved exactly. The first is where $\alpha_P = \alpha_M$, but the associated coupling constants g_P and g_M (defined in Sec. II) are different. The second case arises when α_P and α_M differ, but $g_P = 0$, so that the Pomeranchuk trajectory never emits particles. In both of these cases, one of the effects of summing over all poles is to introduce an infinite number of unitarity cuts spaced apart by $\alpha_P - 1$. If $\alpha_P = 1$, these cuts all coalesce. A similar phenomenon occurs for the poles.

In the first soluble case, if $\alpha_P = 1$, the summation over nonleading poles produces an energy-independent phase which is the leading behavior of the elastic S -matrix element, and a constant total cross section emerges. In the second case a similar phenomenon occurs if $\alpha_P = 1$ and $\alpha_M < 1 + g_M^2$. Since a phase satisfies elastic unitarity, in this situation there is no particle production to leading order in energy. However, this phase does change the conclusion of I that the multi-Regge region of phase space always gives an energy-decreasing contribution to the total cross section if the input trajectory is unity or less. If, on the other hand, $\alpha_M > 1 + g_M^2$, particle production does occur. The elastic cross section, however, would then necessarily be larger than one-half of the total cross section.

The outline of the paper is as follows. In Sec. II the CP model is written down in the notation of I. The Z operator, defined in I, which takes into account emission or absorption of any number of

pions from one chain, is specified for the CP model. As an illustration, the elastic scattering amplitude arising from exchange of two chains is calculated.

Amplitudes involving more than two chains are complicated by the combinatorial complexity. The powerful Green's-function method of I is introduced in Sec. III to carry out these calculations, and the necessary N -chain Hamiltonian H_N is derived. The bound states of the N -chain Hamiltonian are the Regge poles arising from N -chain exchange. In Sec. IV the soluble cases are discussed in detail for two-chain exchange. In Sec. V this discussion is generalized to N chains, and the sum over N is carried out. The J -plane structure of the resulting amplitude is also discussed in Sec. V. In Sec. VI the inclusive and exclusive cross sections are briefly discussed, and in Sec. VII a short summary is given. In an Appendix, a proof is given that both leading and nonleading poles grow with N like N^2 .

II. UNITARIZED CHEW-PIGNOTTI MODEL

The kinematics is defined in Fig. 2. Working in the center-of-mass system, with the beam direction along the Z axis, a general four-vector q , with $q^2 = m^2$, can be specified by its momentum in the x - y plane, \vec{q} , and its rapidity,

$$y = \frac{1}{2} \ln \left(\frac{q_0 + q_z}{q_0 - q_z} \right). \quad (1)$$

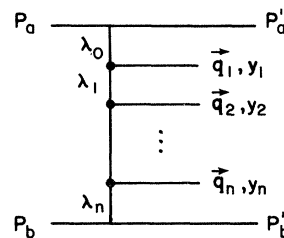
The Mandelstam variable $s = (p_a + p_b)^2 = M^2 e^Y$, where M is the proton mass. The kinematic variables will be taken as Y ,

$$\vec{\Delta} = \frac{1}{2}(\vec{p}'_a - \vec{p}_a) - \frac{1}{2}(\vec{p}'_b - \vec{p}_b), \quad (2)$$

and the pion coordinates q_i, y_i .

In I, it was shown that the S matrix is diagonal in \vec{B} , the coordinate conjugate to $\vec{\Delta}$. Note that for elastic scattering $\vec{\Delta} = \vec{p}'_a - \vec{p}_a$, and hence the momentum transfer $t = (p_a - p'_a)^2 = -\vec{\Delta}^2$ when s is large.

The basic input is the amplitude W_n for the scattering process shown in Fig. 2. Following CP, the scattering occurs by exchange of a fixed pole α_λ , with $\lambda = P$ or M . The vertex function is taken to be

FIG. 2. The amplitude W_n .

separable, i.e., if a pole of type λ converts to a pole λ' by emitting a pion with transverse momentum q , rapidity y [Fig. 3(a)], the vertex function will be taken as $g_{\lambda\lambda'}g_{\lambda'}g(q)$.⁴ If the two protons are separated by impact parameter \vec{B} , the coupling of a trajectory of type λ to the proton will be $h_{\lambda}(\vec{B})$. Therefore the amplitude for the process shown in Fig. 2 is

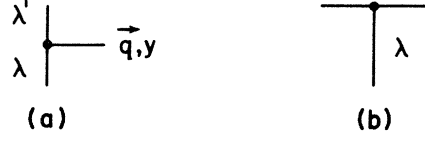


FIG. 3. Vertex functions.

$$\int d^2B e^{-i\vec{B}\cdot\vec{\Delta}} \tilde{\Delta} W_n(Y, \vec{B}; \vec{q}_i, y_i) = \int d^2B e^{-i\vec{B}\cdot\vec{\Delta}} h_{\lambda_0}(\vec{B}) \prod_{i=0}^n \{ \exp[\alpha_{\lambda_i}(y_i - y_{i+1})] \theta(y_i - y_{i+1}) \} \prod_{i=1}^n [g(\vec{q}_i) g_{\lambda_{i-1}} g_{\lambda_i}] h_{\lambda_n}(\vec{B}), \quad (3)$$

where $y_0 = -y_{n+1} = \frac{1}{2}Y$ in the center-of-mass system. The operator Z_n defined in I, which handles emission or absorption of n pions, is then

$$Z_n(Y, \vec{B}) = e^{-Y} \sum_{\lambda_0, \dots, \lambda_n} \int \prod_{i=1}^n \frac{d^2q_i}{(2\pi)^2} \int_{-Y/2}^{Y/2} \prod_{i=1}^n \frac{dy_i}{4\pi} W_n(Y, \vec{B}; y_i, \vec{q}_i, \lambda_i) : \prod_{i=1}^n [a(\vec{q}_i, y_i) + a^\dagger(-\vec{q}_i, y_i)] :. \quad (4)$$

The sum in Eq. (2) runs over $\lambda_i = P$ or M . In Eq. (4), $a^\dagger(\vec{q}, y)$ is an operator which creates a pion of transverse momentum \vec{q} , rapidity y , when acting on the "vacuum," which is the 2-proton state. The commutation relation is $[a(\vec{q}, y), a^\dagger(\vec{q}', y')] = (2\pi)^2 4\pi \delta^2(\vec{q} - \vec{q}') \delta(y - y')$.

To simplify these formulas a bit, define

$$A(y) = \int \frac{d^2\vec{q}}{(2\pi)^2} g(\vec{q}) a(\vec{q}, y). \quad (5)$$

Normalizing $g(q)$ so that

$$\int \frac{d^2\vec{q}}{(2\pi)^2} g^2(\vec{q}) = 1,$$

then $[A(y), A^\dagger(y')] = 4\pi \delta(y - y')$. Z_n may then be rewritten as

$$Z_n(Y, \vec{B}) = e^{-Y} \sum_{\lambda_0, \dots, \lambda_n} \int_{-Y/2}^{Y/2} \prod_{i=1}^n \frac{dy_i}{4\pi} \hat{W}_n(Y, \vec{B}; y_i; \lambda_i) : \prod_{i=1}^n [A(y_i) + A^\dagger(y_i)] : , \quad (6)$$

where

$$\hat{W}_n(Y, \vec{B}; y_i; \lambda_i) = h_{\lambda_0}(\vec{B}) \prod_{i=1}^n \exp[\alpha_{\lambda_i}(y_i - y_{i+1})] \theta(y_i - y_{i+1}) \prod_{i=1}^n (g_{\lambda_{i-1}} g_{\lambda_i}) h_{\lambda_n}(\vec{B}). \quad (7)$$

For the case where no pions are emitted,

$$Z_0(Y, \vec{B}) = e^{-Y} \sum_{\lambda_0} h_{\lambda_0}^2(\vec{B}) \exp(\alpha_{\lambda_0} Y). \quad (8)$$

In impact-parameter space the S operator is given by

$$S(Y, \vec{B}) = \exp[iZ(Y, \vec{B})],$$

where

$$Z(Y, \vec{B}) = \sum_{n=0}^{\infty} Z_n(Y, \vec{B}). \quad (9)$$

It is now a straightforward matter to compute the contribution to the elastic S-matrix element arising from ladder graphs (two-chain exchange) (Fig. 4):

$$S_{22}^{\text{ladder}}(Y, \vec{B}) = \frac{i^2}{2!} \langle 0 | Z^2(Y, \vec{B}) | 0 \rangle = \frac{(i)^2}{2!} \sum_{n=0}^{\infty} \langle 0 | Z_n^2 | 0 \rangle. \quad (10)$$

For $n \geq 2$ one finds

$$\frac{i^2}{2!} \langle 0 | Z_n^2 | 0 \rangle = \frac{(i)^2}{2!} e^{-2Y} \int \prod_{i=1}^n \frac{dy_i}{4\pi} \sum_{\lambda_0, \dots, \lambda_n} \sum_{\lambda'_0, \dots, \lambda'_n} \hat{W}_n(Y; \vec{B}; y_i; \lambda_i) \hat{W}_n(Y; \vec{B}; y_i; \lambda'_i). \quad (11)$$

Introducing $x_i = y_i - y_{i+1}$, $i=0, 1, \dots, n$, this can be rewritten

$$\frac{i^2}{2!} \langle 0 | Z_n^2 | 0 \rangle = \frac{i^2}{2!} e^{-2Y} \int_0^\infty \prod_{i=0}^n \frac{dx_i}{4\pi} 4\pi \delta(\sum x_i - Y) \left(\sum_{\lambda_0, \lambda'_0} h_{\lambda_0}(\vec{B}) h_{\lambda'_0}(\vec{B}) g_{\lambda_0} g_{\lambda'_0} \exp[\alpha_{\lambda_0} + \alpha_{\lambda'_0} x_0] \right) \\ \times \left(\prod_{i=1}^{n-1} \sum_{\lambda_i, \lambda'_i} g_{\lambda_i}^2 g_{\lambda'_i}^2 \exp[(\alpha_{\lambda_i} + \alpha_{\lambda'_i}) x_i] \right) \left(\sum_{\lambda_n, \lambda'_n} h_{\lambda_n}(\vec{B}) h_{\lambda'_n}(\vec{B}) g_{\lambda_n} g_{\lambda'_n} \exp[(\alpha_{\lambda_n} + \alpha_{\lambda'_n}) x_n] \right). \quad (12)$$

Taking the Laplace transform,

$$\int_0^\infty dY \frac{i^2}{2!} e^{-iY} \langle 0 | Z_n^2(Y, \vec{B}) | 0 \rangle = \frac{4\pi}{2!} (i)^2 H^2(l, \vec{B}) X(l)^{n-1}, \quad (13)$$

where

$$H(l, \vec{B}) = \frac{1}{4\pi} \sum_{\lambda, \lambda'} \frac{h_\lambda(\vec{B}) h_{\lambda'}(\vec{B}) g_\lambda g_{\lambda'}}{l+2 - \alpha_\lambda - \alpha_{\lambda'}}, \quad (14)$$

$$X(l) = \frac{1}{4\pi} \sum_{\lambda, \lambda'} \frac{g_\lambda^2 g_{\lambda'}^2}{l+2 - \alpha_\lambda - \alpha_{\lambda'}}.$$

Taking into account the cases $n=0, 1$, the Mellin transform of $S_{22}^{\text{ladder}}(Y, \vec{B})$ is therefore

$$\tilde{S}_{22}^{\text{ladder}}(l, \vec{B}) = \int_0^\infty dY e^{-iY} S_{22}^{\text{ladder}}(Y, \vec{B}) \\ = \frac{4\pi}{2} \left(\frac{i}{2} \right)^2 \{ M_1(l, \vec{B}) + H(l, \vec{B}) [1 - X(l)]^{-1} \}, \quad (15)$$

where $M_1(l, \vec{B})$, which arises from exchange of two trajectories with no pions produced, is

$$M_1(l, \vec{B}) = \frac{1}{4\pi} \sum_{\lambda, \lambda'} \frac{h_\lambda^2(\vec{B}) h_{\lambda'}^2(\vec{B})}{l+2 - \alpha_\lambda - \alpha_{\lambda'}}. \quad (16)$$

The dynamical output poles are determined by the cubic equation

$$1 = X(l) \\ = \frac{1}{4\pi} \left(\frac{g_P^4}{l+2 - 2\alpha_P} + \frac{2g_P^2 g_M^2}{l+2 - \alpha_P - \alpha_M} + \frac{g_M^4}{l+2 - 2\alpha_M} \right). \quad (17)$$

The poles of $M_1(l, \vec{B})$ at $l+2 = \alpha_\lambda + \alpha_{\lambda'}$ will in general occur as output poles, though in special cases these may be canceled by the term $[H(l, \vec{B})]^2$

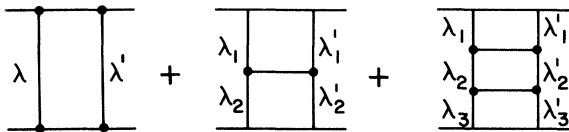


FIG. 4. Ladder graphs.

$\times [1 - X(l)]^{-1}$. These poles would be two-Reggeon cuts in a model where the Regge poles are moving.

A detailed discussion of these results will be postponed until Sec. IV.

III. A t -CHANNEL INTEGRAL EQUATION

A t -channel integral equation similar to that derived in Sec. IV of I may be used to sum the series in Eq. (15). The advantage of the integral equation is that it easily generalizes to N chains. The situation is complicated here by the fact that the Reggeons on either side of the ladder can be P or M trajectories. Thus each Reggeon can be thought of as a two-state, or spin- $\frac{1}{2}$ system.

Consider Fig. 5, which is a section of one of the ladder graphs in Fig. 4. As may be seen from Eqs. (12)–(14), the free propagation of Reggeons 1 and 2, in states λ_1 and λ_2 , is represented by a factor $(4\pi)^{-1} (l+2 - \alpha_{\lambda_1} - \alpha_{\lambda_2})^{-1}$. Define single-Reggeon state vectors $|+\rangle$ and $|-\rangle$, where $|+\rangle$ and $|-\rangle$ correspond to P and M . The two-Reggeon state is $|\lambda_1 \lambda_2\rangle$. (The labels $+$ and P are here interchangeable, as are $-$ and M .) Define the single-particle spin operator J_z by

$$J_z |\pm\rangle = \pm \frac{1}{2} |\pm\rangle, \quad (18)$$

and also define $J_z^{(2)} = J_{z,1} + J_{z,2}$, where $J_{z,i}$ is J_z for Reggeon i . The free-particle propagator can be written

$$G_0^{(2)} = \frac{1}{4\pi} (l - H_0^{(2)})^{-1} \\ = \frac{1}{4\pi} \left[l+2 - \alpha_P \sum_{i=1}^2 \left(\frac{1}{2} + J_{z,i} \right) - \alpha_M \sum_{i=1}^2 \left(\frac{1}{2} - J_{z,i} \right) \right]^{-1} \\ = \frac{1}{4\pi} [l+2 - (\alpha_P + \alpha_M) - (\alpha_P - \alpha_M) J_z^{(2)}]^{-1}. \quad (19)$$

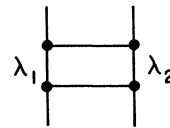


FIG. 5. A section of a ladder.

For N Reggeons this generalizes to

$$G_0^{(N)} \equiv \frac{1}{4\pi} (l - H_0^{(N)})^{-1} \\ = \frac{1}{4\pi} [l + N - \frac{1}{2}N(\alpha_P + \alpha_M) - (\alpha_P - \alpha_M)J_z^{(N)}]^{-1}, \quad (20)$$

with

$$J_z^{(N)} = \sum_{i=1}^N J_{z,i}.$$

The two-body potential between Reggeons 1 and 2 is an operator V_{12} which produces a transition from $|\lambda_1\lambda_2\rangle$ to $|\lambda'_1\lambda'_2\rangle$ with amplitude $g_{\lambda'_1\lambda'_2}g_{\lambda_1\lambda_2}$. Thus

$$V_{12} = \sum_{\lambda'_1, \lambda'_2, \lambda_1, \lambda_2} g_{\lambda'_1\lambda'_2}g_{\lambda_1\lambda_2} |\lambda'_1\lambda'_2\rangle \langle \lambda_1\lambda_2|. \quad (21)$$

Writing the projection operators in Eq. (21) in terms of the angular momentum operators $J_{x,i}$, $J_{y,i}$ and $J_{z,i}$, V_{12} becomes

$$V_{12} = [\frac{1}{2}(g_P^2 + g_M^2) + (g_P^2 - g_M^2)J_{z,1} + 2g_P g_M J_{x,1}] \\ \times [\frac{1}{2}(g_P^2 + g_M^2) + (g_P^2 - g_M^2)J_{z,2} + 2g_P g_M J_{x,2}]. \quad (22)$$

The two-body full Green's function satisfies

$$G^{(2)} = G_0^{(2)} + G_0^{(2)} V_{12} G^{(2)}. \quad (23)$$

Defining the full two-body Hamiltonian $H^{(2)}$ by $G^{(2)} = (4\pi)^{-1}(l - H^{(2)})^{-1}$, then

$$H^{(2)} = H_0^{(2)} + \frac{1}{4\pi} V_{12}. \quad (24)$$

To generalize this discussion to N Reggeons, define the potential

$$V^{(N)} = \sum_{r=2}^N \sum_{s=1}^{r-1} V_{rs}, \quad (25)$$

with V_{rs} defined by an equation similar to Eq. (22). The N -body full Hamiltonian is

$$H^{(N)} = H_0^{(N)} + \frac{1}{4\pi} V^{(N)}. \quad (26)$$

Finally, the N -body Green's function $G^{(N)}$ is defined as

$$G^{(N)} = \frac{1}{4\pi} (l - H^{(N)})^{-1}. \quad (27)$$

Now consider Fig. 6, which represents Reggeons λ_1 and λ_2 attaching to the proton. A moment's thought shows that the appropriate factor $h_{\lambda_1}(\vec{\mathbb{B}}) \times h_{\lambda_2}(\vec{\mathbb{B}})$ is obtained when the diagonal matrix element

$$\langle h^{(2)}(\vec{\mathbb{B}}) | G^{(2)}(l) | h^{(2)}(\vec{\mathbb{B}}) \rangle$$

is computed, where

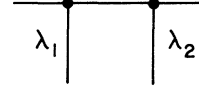


FIG. 6. Attaching the ladder.

$$|h^{(2)}(\vec{\mathbb{B}})\rangle = \sum_{\lambda_1, \lambda_2} h_{\lambda_1}(\vec{\mathbb{B}}) h_{\lambda_2}(\vec{\mathbb{B}}) |\lambda_1\lambda_2\rangle. \quad (28)$$

Thus,

$$\tilde{S}_{22}^{\text{ladder}}(l, \vec{\mathbb{B}}) = \frac{4\pi}{2!} (i)^2 \langle h^{(2)}(\vec{\mathbb{B}}) | G^{(2)}(l) | h^{(2)}(\vec{\mathbb{B}}) \rangle. \quad (29)$$

For N -chain exchange the general result is

$$\tilde{S}_{22}^{(N)}(l, \vec{\mathbb{B}}) = \frac{4\pi}{N!} (i)^N \langle h^{(N)}(\vec{\mathbb{B}}) | G^N(l) | h^{(N)}(\vec{\mathbb{B}}) \rangle, \quad (30)$$

with $|h^{(N)}(\vec{\mathbb{B}})\rangle$ the obvious generalization of $|h^{(2)}(\vec{\mathbb{B}})\rangle$. The inverse Laplace transform of Eq. (30) is

$$S_{22}^{(N)}(Y, \vec{\mathbb{B}}) = \frac{1}{N!} (i)^N \langle h^N(\vec{\mathbb{B}}) | e^{YH^{(N)}} | h^N(\vec{\mathbb{B}}) \rangle, \quad (31)$$

which explicitly shows that the eigenstates of $H^{(N)}$ are output Regge poles in $S_{22}^{(N)}(Y, \vec{\mathbb{B}})$.

IV. DIAGONALIZATION OF $H^{(2)}$

The diagonalization of $H^{(N)}$ is difficult to carry out in general. Even the case $N=2$ is a bit complicated. For any N , $H^{(N)}$ has 2^N eigenstates, and thus there are four eigenstates for $H^{(2)}$. Of these, one is antisymmetric and three are symmetric under interchange of Reggeon 1 with Reggeon 2. The antisymmetric state, which turns out to be at $l = \alpha_P + \alpha_M - 2$, independent of the coupling constants, does not occur in S_{22}^{ladder} , because $|h^{(2)}(\vec{\mathbb{B}})\rangle$ is symmetric. $H^{(2)}$ can be diagonalized in the symmetric subspace; the resulting eigenvalue equation is equivalent to Eq. (17).

For certain values of the parameters, however, $H^{(N)}$ can be exactly diagonalized. To see this, note that

$$(g_P^2 - g_M^2)J_z + 2g_P g_M J_x = (g_P^2 + g_M^2)(\cos\theta J_z + \sin\theta J_x), \quad (32)$$

where

$$\cos\theta = \frac{g_P^2 - g_M^2}{g_P^2 + g_M^2}, \\ \sin\theta = \frac{2g_P g_M}{g_P^2 + g_M^2}. \quad (33)$$

Defining

$$\tilde{J}_z = \cos\theta J_z + \sin\theta J_x \\ = e^{-i\theta J_y} J_z e^{i\theta J_y}, \quad (34)$$

then

$$V_{12} = \frac{(g_P^2 + g_M^2)^2}{16\pi} (1 + 2\bar{J}_{z,1}) (1 + 2\bar{J}_{z,2}). \quad (35)$$

Using (34), J_z can be rewritten as

$$\bar{J}_z = \cos\theta \bar{J}_z - \sin\theta \bar{J}_x, \quad (36)$$

and therefore

$$H^{(2)} = (\alpha_P + \alpha_M - 2) + (\alpha_P - \alpha_M)(\cos\theta \bar{J}_z - \sin\theta \bar{J}_x) + \frac{(g_P^2 + g_M^2)^2}{16\pi} (1 + 2\bar{J}_{z,1})(1 + 2\bar{J}_{z,2}). \quad (37)$$

Clearly, there are two cases where $H^{(2)}$ can be exactly diagonalized, namely, $\alpha_P = \alpha_M$, or $\sin\theta = 0$, for in these cases \bar{J}_x drops out entirely. The eigenstates of $H^{(2)}$ will then have the form $|\bar{\lambda}_1 \bar{\lambda}_2\rangle$, where

$$|\bar{\lambda}\rangle = e^{-i\theta J_y} |\lambda\rangle. \quad (38)$$

For example, if $\alpha_P = \alpha_M = \alpha$, the highest eigenstate $|\bar{+}\bar{+}\rangle$ has energy

$$E = 2(\alpha - 1) + \frac{(g_P^2 + g_M^2)^2}{4\pi}, \quad (39)$$

and the three lowest states $|\bar{+}\bar{-}\rangle$, $|\bar{-}\bar{+}\rangle$, and $|\bar{-}\bar{-}\rangle$ all have energy $E = 2(\alpha - 1)$, since V_{12} vanishes for these states. To compute the expectation value needed in Eq. (29), note that

$$h_P |+\rangle + h_M |-\rangle = \bar{h}_P |\bar{+}\rangle + \bar{h}_M |\bar{-}\rangle, \quad (40)$$

where

$$\begin{aligned} \bar{h}_P &= h_P \cos\frac{1}{2}\theta + h_M \sin\frac{1}{2}\theta, \\ \bar{h}_M &= h_M \cos\frac{1}{2}\theta - h_P \sin\frac{1}{2}\theta, \\ \cos\frac{1}{2}\theta &= \frac{g_P}{(g_P^2 + g_M^2)^{1/2}}, \\ \sin\frac{1}{2}\theta &= \frac{g_M}{(g_P^2 + g_M^2)^{1/2}}. \end{aligned} \quad (41)$$

Therefore,

$$|h^{(N)}(\vec{B})\rangle = \sum_{\lambda_1, \dots, \lambda_N} \bar{h}_{\lambda_1}(\vec{B}) \cdots \bar{h}_{\lambda_N}(\vec{B}) |\bar{\lambda}_1, \dots, \bar{\lambda}_N\rangle. \quad (42)$$

The function

$$\langle h^{(2)}(\vec{B}) | G^{(2)}(l) | h^{(2)}(\vec{B}) \rangle,$$

then, has a pole at $l = 2(\alpha - 1) + (g_P^2 + g_M^2)^2 / 4\pi$, with residue $[\bar{h}_P(\vec{B})]^4$, and a pole at $l = 2(\alpha - 1)$, with residue $[2\bar{h}_P^2(\vec{B})\bar{h}_M^2(\vec{B}) + \bar{h}_M^4(\vec{B})]$. This is in agreement with a direct calculation using Eq. (15). Note that the pole at $l = 2(\alpha - 1)$ in $S_{22}^{\text{ladder}}(l, \vec{B})$, which would be a two-Reggeon cut if the input poles were

$$S_{22}^{(N)}(Y, \vec{B}) = i^N \sum_{r=0}^N \frac{[h_P^2(\vec{B})]^r}{r!} \frac{[h_M^2(\vec{B})]^{N-r}}{(N-r)!} \exp\left\{Y \left[(N-r)(\alpha_M - 1) + r(\alpha_P - 1) + \frac{g_M^4}{8\pi} (N-r)(N-r-1) \right]\right\}. \quad (46)$$

Summing Eq. (46) over N , one obtains⁵

not fixed, in general has a nonvanishing residue.

A second case when $H^{(2)}$ is exactly diagonalizable occurs when $g_P = 0$, so that $\sin\theta = 0$ and $\cos\theta = -1$. In this case $\bar{h}_P = h_M$ and $\bar{h}_M = -h_P$, and so

$$\langle h^{(2)}(\vec{B}) | G^{(2)}(l) | h^{(2)}(\vec{B}) \rangle$$

has a pole at $2(\alpha_M - 1) + g_M^4 / 4\pi$ with residue h_M^4 , a pole at $(\alpha_P + \alpha_M - 2)$ with residue $2h_P^2 h_M^2$, and a pole at $2(\alpha_P - 1)$ with residue h_P^4 .

V. EXACTLY SOLUBLE EXAMPLE

In the two cases discussed in Sec. IV, $H^{(N)}$ is exactly diagonalizable for all N . In the following discussion only the case $g_P = 0$ will be treated explicitly; the results for the case $\alpha_P = \alpha_M$ will be mentioned at the end. This case was chosen for detailed study because when $g_P = 0$ the ladder diagrams of this model precisely correspond to one of the cases studied by CP. In general, CP allow only the transitions $P \rightarrow M$, $M \rightarrow P$, and $M \rightarrow M$. However, in the case chosen by them to compare with experiment, they allow only $M \rightarrow M$ and set the other transition probabilities to zero. Thus, their ladder diagrams have only meson trajectories as rungs; in the present model this occurs when $g_P = 0$.

When $g_P = 0$, $H^{(N)}$ has the form

$$H^{(N)} = \frac{1}{2} N(\alpha_P + \alpha_M - 2) - (\alpha_P - \alpha_M) J_z + \frac{g_M^4}{16\pi} \sum_{r=2}^N \sum_{s=1}^{r-1} (1 + 2J_{z,r})(1 + 2J_{z,s}). \quad (43)$$

All eigenstates of $H^{(N)}$ are of the form $|\bar{\lambda}_1, \bar{\lambda}_2, \dots, \bar{\lambda}_N\rangle$. Let $|N, r\rangle$ denote any of the $N! / r!(N-r)!$ eigenstates, where r λ 's are $-$ and $(N-r)$ λ 's are $+$. Since the operator $1 + 2\bar{J}_z$ vanishes when applied to the state $|\bar{-}\rangle$, the potential $V^{(N)}$ effectively counts the number of pairs of $+$'s. Thus $|N, r\rangle$ has energy $E_{N,r}$

$$E_{N,r} = \frac{1}{2} N(\alpha_P + \alpha_M - 2) - (\alpha_P - \alpha_M) \frac{1}{2} (N - 2r) + \frac{g_M^2}{4\pi} (N - r) \frac{1}{2} (N - r - 1). \quad (44)$$

Also

$$\begin{aligned} \langle \bar{h}^{(N)}(\vec{B}) | N, r \rangle &= [(\bar{h}_-(B))^r (\bar{h}_+(B))^{N-r}] \\ &= [-h_P(B)]^r [h_M(B)]^{N-r}. \end{aligned} \quad (45)$$

Using Eq. (31) and taking into account the degeneracy of $|N, r\rangle$,

$$\begin{aligned}
S_{22}(Y, \vec{B}) &= \sum_{r=0}^{\infty} [i h_P^2(\vec{B})]^r e^{Yr(\alpha_P - 1)} \sum_{N=r}^{\infty} \frac{[i h_M^2(\vec{B})]^{N-r}}{(N-r)!} \exp\left\{Y\left[(N-r)(\alpha_M - 1) + \frac{g_M^4}{8\pi}(N-r)(N-r-1)\right]\right\} \\
&= \exp[i h_P^2(\vec{B})e^{Y(\alpha_P - 1)}] \sum_{N=0}^{\infty} \frac{[i h_M^2(\vec{B})]^N}{N!} \exp\left\{Y\left[\left(\alpha_M - 1 - \frac{g_M^4}{8\pi}\right)N + N^2 \frac{g_M^4}{8\pi}\right]\right\}. \quad (47)
\end{aligned}$$

It follows from Eq. (44) that for N sufficiently large, the eigenvalue $E_{N,0}$ is the leading pole, $E_{N,1}$ is the next-to-leading pole, etc. Thus the first term in the sum over r in Eq. (47) is the sum over leading poles (for N large), the next term is the sum over next-to-leading poles, etc. For fixed r , $E_{N,r}$ grows with N like N^2 and thus the sum over N for fixed r diverges. The divergent power series in Eq. (47) is, however, precisely the elastic S -matrix element calculated in I, i.e., it is the sum of all checkerboard graphs with only the meson trajectory α_M exchanged. According to I, it should be interpreted via the "Gaussian integral trick": In Eq. (47) use the identity

$$e^{N^2 g^2 Y} = \frac{1}{\sqrt{\pi}} \int_{-\infty}^{+\infty} dx e^{-x^2} e^{2NgY^{1/2}x}, \quad (48)$$

and do the sum over N before doing the x integral. The result is

$$S_{22}(Y, \vec{B}) = \exp[i h_P^2(\vec{B})e^{(\alpha_P - 1)Y}] S_{22}^M(Y, \vec{B}), \quad (49)$$

where

$$\begin{aligned}
S_{22}^M(Y, \vec{B}) &= \frac{1}{\sqrt{\pi}} \int_{-\infty}^{+\infty} dx e^{-x^2} \\
&\quad \times \exp[i h_M^2(\vec{B})e^{Y(\alpha_M - 1 - g^2) + gY^{1/2}x}], \quad (50)
\end{aligned}$$

with

$$g = \frac{g_M^2}{\sqrt{8\pi}}.$$

The phase factor $\exp(i h_P^2(\vec{B})e^{(\alpha_P - 1)Y})$ has a transparent physical interpretation. Since the Pomeron trajectory never emits pions when $g_P = 0$, it couples only by repeated exchange between the protons. Consider any checkerboard diagram involving N chains of α_M exchange [Fig. 7(a)]. The effect of exchanging L Pomeron trajectories in all possible ways in addition to the meson exchange [Fig. 7(b)] is to multiply the diagram of Fig. 7(a) by a factor $(i h_P^2 e^{(\alpha_P - 1)Y})^L / L!$. Summing over L , the phase factor in Eq. (49) emerges.

Now consider the J -plane structure of $S_{22}(Y, \vec{B})$. As shown in I, if $\alpha_M < 1 + g^2$, $S_{22}^M(Y, \vec{B})$ has poles at $J = \alpha_N = N(\alpha_M - 1) + N(N - 1)g^2$ for all non-negative integers $N \leq N_0 = (1 + g - \alpha_M)/2g^2$, and a cut at $J = \alpha_c = -(1 + g^2 - \alpha_M)^2/g^2$. Expanding the phase in Eq. (49) in a power series, $S_{22}(Y, \vec{B})$ clearly has poles at the points $J = \alpha_N + L(\alpha_P - 1)$ and cuts at the points $J = \alpha_c + L(\alpha_P - 1)$, with L a non-negative integer. If $\alpha_P = 1$, the cuts all coalesce into a single cut at α_c , and a similar thing happens with the poles.

One of the most interesting features of S_{22}^M , as discussed in I, is that when a pole α_N collides with the cut α_c (as a result of varying g), the pole

is forced onto an unphysical sheet. Clearly, in this case, when a pole at $\alpha_N + L(\alpha_P - 1)$ collides with the cut at $\alpha_c + L(\alpha_P - 1)$, the pole is forced onto an unphysical sheet. However, collisions between the pole at $\alpha_N + L(\alpha_P - 1)$ and the cut at $\alpha_c + L'(\alpha_P - 1)$, where $L' \neq L$, have no effect on the pole.

When $\alpha_M < 1 + g^2$ the leading pole in S_{22}^M is at $J = 0$ ($N = 0$) and S_{22}^M approaches unity for large Y . Thus, for large Y ,

$$S_{22}(Y, \vec{B}) \rightarrow \exp[i h_P^2(\vec{B})e^{(\alpha_P - 1)Y}]. \quad (51)$$

Note that the phase factor in Eq. (51) arises from the sum over r in Eq. (47), i.e., the sum over non-leading poles.

The total and elastic cross sections, in the normalization of I, are

$$\begin{aligned}
\sigma_{\text{tot}} &= 2 \int d^2B \operatorname{Re}[1 - S_{22}(Y, \vec{B})], \\
\sigma_{\text{el}} &= \int d^2B |1 - S_{22}(Y, \vec{B})|^2. \quad (52)
\end{aligned}$$

Since S_{22} is just a phase, $\sigma_{\text{tot}} = \sigma_{\text{el}}$ to leading order

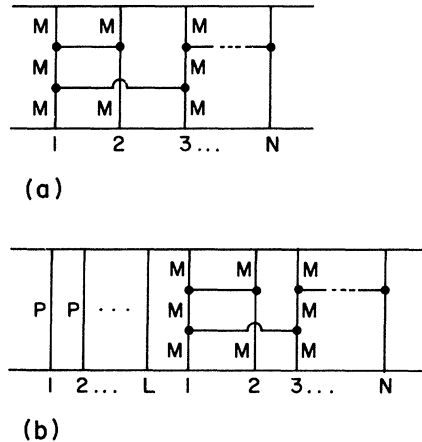


FIG. 7. The modification of a meson checkerboard graph by Pomeron trajectory exchange.

in s , and

$$\begin{aligned} \sigma_{\text{tot}} &\sim e^{2(\alpha_P - 1)Y} \int d^2B h_P^4(\vec{B}) \quad (\alpha_P < 1) \\ &\sim 2 \int d^2B [1 - \cosh h_P^2(\vec{B})] \quad (\alpha_P = 1). \end{aligned} \quad (53)$$

When $\alpha_P > 1$, the energy dependence of σ_{tot} depends on $h_P(\vec{B})$. If $h_P(\vec{B}) = h e^{-B/2R_0}$, then⁶

$$\sigma_{\text{tot}} \sim 2\pi R_0^2 (\alpha_P - 1)^2 Y^2. \quad (54)$$

If $\alpha_M > 1 + g^2$ (Ref. 7), the total and elastic cross sections will no longer be equal. As one example, which is illustrated in Fig. 8, suppose that $\alpha_P = 1$,

$$h_P(\vec{B}) = h_P \theta(B_P - |\vec{B}|), \quad (55)$$

$$h_M(\vec{B}) = h_M \theta(B_M - |\vec{B}|),$$

where $B_M < B_P$.⁸ Using the techniques of I it can be shown that, due to the rapid oscillations in the integrand of Eq. (50), $S_{22}^M(Y, \vec{B}) = 0$ when $|\vec{B}| < B_M$, whereas clearly $S_{22}^M(Y, \vec{B}) = 1$ for $|\vec{B}| > B_M$. In other words, the incoming wave is completely absorbed when $|\vec{B}| < B_M$. For $B_M < |\vec{B}| < B_P$ elastic scattering occurs, and therefore

$$\begin{aligned} \sigma_{\text{tot}} &= 2\pi B_M^2 + 2\pi(B_P^2 - B_M^2)(1 - \cosh h_P^2), \\ \sigma_{\text{tot}} - \sigma_{\text{el}} &= \pi B_M^2. \end{aligned} \quad (56)$$

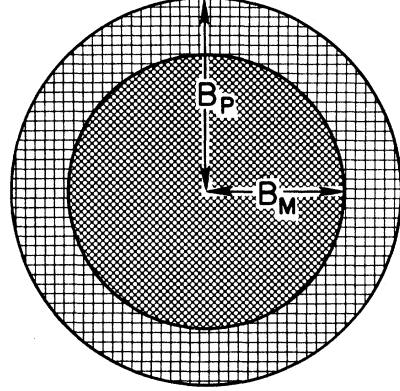


FIG. 8. In the inner shaded disk of radius B_M the incoming two particle state is completely absorbed and pion production occurs. In the cross-hatched region the incoming state is scattered elastically.

All of the particle production comes from the region $|\vec{B}| < B_M$, where S_{22} vanishes. It follows from Eq. (53) that $\sigma_{\text{tot}} > \sigma_{\text{el}} > \frac{1}{2}\sigma_{\text{tot}}$, and that σ_{el} and σ_{tot} are constants.

Very similar results occur in the other soluble case $\alpha_P = \alpha_M = \alpha$. For example, the elastic S -matrix element is

$$S_{22}(Y, \vec{B}) = \exp(i\tilde{h}_+ B^2) e^{(\alpha - 1)Y} \sum_{N=0}^{\infty} \frac{(i\tilde{h}_+(\vec{B}))^N}{N!} \exp\{Y[(\alpha - 1 - \tilde{g}^2)N + N^2 \tilde{g}^2]\}, \quad (57)$$

where $\tilde{g}^2 = (g_P^2 + g_M^2)/8\pi$. The sum in Eq. (57) is to be interpreted by the Gaussian integral trick. In this case, $\alpha = 1$ implies $\sigma_{\text{tot}} = \sigma_{\text{el}} = \text{constant}$. In both of the soluble cases the extra phase factor changes the conclusion of I that the multi-Regge region gives an energy-decreasing contribution to σ_{tot} if the input trajectory is one or less.

VI. INCLUSIVE AND EXCLUSIVE CROSS SECTIONS

In this section the inclusive and exclusive cross sections will be briefly discussed for the soluble cases. These can all be deduced algebraically, so as a first step certain commutators will be evaluated.

When $g_P = 0$, for $n \geq 2$, Z_n simplifies to

$$Z_n = e^{(\alpha_M - 1)Y} [h_M(\vec{B})]^2 (g_M^2)^{n+1} \frac{1}{n!} \int_{-Y/2}^{Y/2} \prod_{i=1}^n \frac{dy_i}{4\pi} : \prod_{j=1}^n [A(y_j) + A^\dagger(y_j)] :. \quad (58)$$

Therefore

$$[a(\vec{q}, Y), Z_n] = g_M^2 g(\vec{q}) Z_{n-1}, \quad (59)$$

and thus

$$\begin{aligned} [a(\vec{q}, y), Z(Y, \vec{B})] &= g_M^2 g(\vec{q}) [Z - h_P^2(B) e^{(\alpha_P - 1)Y}] \\ &\equiv g_M^2 g(\vec{q}) Z_M. \end{aligned} \quad (60)$$

Z_M , defined in Eq. (60), is the Z operator for meson trajectories alone. Therefore

$$[a(\vec{q}, y), S(Y, \vec{B})] = i g_M^2 g(\vec{q}) S(Y, \vec{B}) Z_M(Y, \vec{B}). \quad (61)$$

The inclusive cross section for one-pion production is

$$\begin{aligned} \frac{d\sigma}{dq} &= \sum_{n=0}^{\infty} \frac{1}{n!} \int d^2B \prod_{i=1}^n dq_i \\ &\quad \times |\langle q, q_1, \dots, q_n | S(Y, \vec{B}) | 0 \rangle|^2, \end{aligned} \quad (62)$$

where the invariant phase space is $dq = d^2q dy / (2(2\pi)^3)$. Reducing out one pion and using completeness and Eq. (30),

$$\begin{aligned}
\frac{d\sigma}{dq} &= \int d^2B \sum_{n=0}^{\infty} \frac{1}{n!} \int \prod_{i=1}^n dq_i \\
&\quad \times |\langle q_1, \dots, q_n | [a(\vec{q}, y), S(Y, \vec{B})] | 0 \rangle|^2 \\
&= \int d^2B \langle 0 | [S^\dagger, a^\dagger] [a, S] | 0 \rangle \\
&= g_M^4 g^2(\vec{q}) \int d^2B \langle 0 | [Z_M(y, \vec{B})]^2 | 0 \rangle \\
&= g_M^4 g^2(\vec{q}) e^{2(\alpha_M - 1 + \varepsilon^2)Y} \int d^2B h_M^4(\vec{B}). \quad (63)
\end{aligned}$$

This is independent of the rapidity of the produced pion, and thus, if $\alpha_M = 1 - g^2$, the multiplicity will grow like logs.

The simplest way to derive the exclusive cross sections is to note that

$$Z(Y, \vec{B}) = h_P^2(\vec{B}) e^{(\alpha_P - 1)Y} + Z_M(Y, \vec{B}), \quad (64)$$

which implies the operator relation⁹

$$S(Y, \vec{B}) = \exp[i h_P^2(\vec{B}) e^{(\alpha_P - 1)Y}] \exp[i Z_M(Y, \vec{B})]. \quad (65)$$

The scattering amplitude operator in \vec{B} space is

$$M(Y, \vec{B}) = 2is [1 - S(Y, \vec{B})].$$

The term $2is$ contributes only for elastic scattering, and hence the phase $\exp[i h_P^2(\vec{B}) e^{(\alpha_P - 1)Y}]$ is irrelevant for the production amplitudes. The production amplitudes are thus identical to those calculated in I, which in fact all vanish at large energy if $\alpha_M < 1 + g^2$. For the case $\alpha_M > 1 + g^2$, the calculation of the production amplitudes seemed too complicated to carry out analytically, and so unfortunately nothing can be said about them here. The cross sections for the other soluble case $\alpha_M = \alpha_P$ can be discussed using similar arguments. A relation analogous to Eq. (65) can also be derived for this case.

VII. SUMMARY AND CONCLUSION

The main point of this work is that the nonleading output Regge pole positions from N chain exchange grow like N^2 and thus are potentially quite important in determining high energy behavior. Their growth with N was shown explicitly in Sec. V in the soluble cases; in the Appendix it is shown in general. The nonleading poles therefore always give rise to unitarity cuts by themselves. In the two exactly soluble cases, summing over the nonleading poles in the case $\alpha_P = 1$ in fact produces an energy-independent phase factor which determines the total cross section at high energy. It is not clear in the general case what the net effect of the nonleading poles will be. Judging

from the soluble cases it seems likely that they will be important.

ACKNOWLEDGMENT

I would like to thank Dr. R. Sugar and Dr. R. Blankenbecler for many hours of enlightenment, and Dr. C. Rosenzweig and Dr. T. Neff for their comments on the manuscript.

APPENDIX

It will be shown here that the leading and non-leading eigenstates of $H^{(N)}$ grow like N^2 . More precisely, denote the eigenvalues of H^N by $E_{N,r}$, with $E_{N,1} \geq E_{N,2} \geq \dots \geq E_{N,N}$. For fixed r , the bounds

$$a_r N + b_r N^2 \leq E_{N,r} \leq a_r' N + b_r' N^2 \quad (A1)$$

will be proven. The main tool will be the minimax principle¹⁰: Let H be a Hermitian operator on an n -dimensional vector space V_n , with eigenvalues $\lambda_1 \geq \lambda_2 \geq \dots \geq \lambda_n$. Let V_r be any r -dimensional subspace of V_n . Then

$$\lambda_r = \max_{V_r} \left[\min_{|\psi\rangle \in V_r} \frac{\langle \psi | H | \psi \rangle}{\langle \psi | \psi \rangle} \right]. \quad (A2)$$

In words, this means pick any subspace V_r , and minimize $\langle \psi | H | \psi \rangle / \langle \psi | \psi \rangle$ over that subspace. Then find the subspace V_r which maximizes the number

$$\min_{\psi \in V_r} \frac{\langle \psi | H | \psi \rangle}{\langle \psi | \psi \rangle}.$$

This maximum is the r th eigenvalue from the top. For $r = N$ the minimax principle is precisely the Rayleigh-Ritz variational method.

Consider first the highest eigenvalue $E_{N,1}$. The minimax principle gives a lower bound: For any $|\psi\rangle$

$$E_{N,1} \geq \frac{\langle \psi | H^{(N)} | \psi \rangle}{\langle \psi | \psi \rangle}. \quad (A3)$$

Now (dropping the \sim for rotational convenience)

$$\begin{aligned}
H^{(N)} &= \frac{1}{2} N(\alpha_P + \alpha_M - 2) \\
&\quad + (\alpha_P - \alpha_M)(\cos \theta J_z - \sin \theta J_x) \\
&\quad + \frac{1}{4} g^2 \sum_{r=2}^N \sum_{s=1}^{r-1} (1 + 2J_{z,r})(1 + 2J_{z,s}), \quad (A4)
\end{aligned}$$

where $g^2 = (g_P^2 + g_M^2)/4\pi$. Choose the state $|\psi\rangle = |+\dots+\rangle$, and note that $\langle +\dots+ | J_x | +\dots+\rangle = 0$. Thus

$$\begin{aligned}
E_{N,1} &\geq \frac{1}{2} N(\alpha_P + \alpha_M - 2) + \frac{1}{2} N(\alpha_P - \alpha_M) \cos \theta \\
&\quad + \frac{1}{2} g^2 N(N-1) \\
&\equiv E_{N,1}^0. \quad (A5)
\end{aligned}$$

To get an upper bound for $E_{N,1}$, split the Hamiltonian into

$$H^{(N)} = \bar{H}^N + \bar{V}^N, \quad (\text{A6})$$

$$\bar{H}^N = \frac{1}{2}N(\alpha_P + \alpha_M - 2) + (\alpha_P - \alpha_M) \cos\theta \bar{J}_z \\ + \frac{1}{4}g^2 \sum_{r=2}^N \sum_{s=1}^{r-1} (1 + 2\bar{J}_{z,r})(1 + 2\bar{J}_{z,s}),$$

$$\bar{V}^N = -(\alpha_P - \alpha_M) \sin\theta \bar{J}_x.$$

Let $|E_{N,1}\rangle$ denote the normalized eigenstate with eigenvalue $E_{N,1}$. Clearly

$$E_{N,1} = \langle E_{N,1} | \bar{H}^N | E_{N,1} \rangle + \langle E_{N,1} | \bar{V}^N | E_{N,1} \rangle. \quad (\text{A7})$$

By the usual rules for adding angular momenta, \bar{J}_x has eigenvalues between $-\frac{1}{2}N$ and $\frac{1}{2}N$, and so

$$\langle E_{N,1} | \bar{V}^N | E_{N,1} \rangle \leq |(\alpha_P - \alpha_M) \sin\theta| \frac{1}{2}N. \quad (\text{A8})$$

Also, expanding $|E_{N,1}\rangle$ in eigenstates of \bar{H}^N , it is clear that $\langle E_{N,1} | \bar{H}^N | E_{N,1} \rangle$ is bounded above by the highest eigenvalue of \bar{H}^N , which is $E_{N,1}^0$. Thus

$$E_{N,1}^0 \leq E_{N,1} \leq E_{N,1}^0 + |(\alpha_P - \alpha_M) \sin\theta| \frac{1}{2}N \quad (\text{A9})$$

as advertised in Eq. (A1).

It is trivial to get an upper bound on $E_{N,r}$, namely, $E_{N,r} \leq E_{N,1}$. To get a lower bound, the minimax principle is needed. As an example, the eigenvalue $E_{N,2}$ will be studied; the same method applies generally. From Eq. (A2), if V_r is any two-dimensional subspace,

$$\lambda_2 \geq \min_{|\psi\rangle \in V_2} \frac{\langle \psi | H | \psi \rangle}{\langle \psi | \psi \rangle}. \quad (\text{A10})$$

Pick the two-dimensional subspace of vectors of the form

$$|\psi\rangle = a | - + + \cdots + \rangle + b | + - + \cdots + \rangle. \quad (\text{A11})$$

Once again, $\langle \psi | J_x | \psi \rangle = 0$, and in fact, $\langle \psi | H | \psi \rangle / \langle \psi | \psi \rangle$ is independent of a and b . Therefore

$$E_{N,2} \geq \frac{1}{2}N(\alpha_P + \alpha_M - 2) + (\alpha_P - \alpha_M) \cos\theta \frac{1}{2}(N-2) \\ + g^2 \frac{1}{2}(N-1)(N-2), \quad (\text{A12})$$

as was to be proven.

*Research supported by the Air Force Office of Scientific Research, Office of Aerospace Research, United States Air Force, under Contract No. F44620-70-C-0028.

¹S. Auerbach, R. Aviv, R. Sugar, and R. Blankenbecler, Phys. Rev. D **6**, 2216 (1972), hereafter referred to as I; S. Auerbach *et al.*, Phys. Rev. Lett. **29**, 522 (1972). For previous work on similar lines, see R. Aviv, R. Sugar, and R. Blankenbecler, Phys. Rev. D **5**, 3252 (1972); G. Calucci, R. Jengo, and C. Rebbi, Nuovo Cimento **4A**, 330 (1970); **6A**, 601 (1971); G. Calucci and R. Jengo, Nuovo Cimento Lett. **4**, 33 (1972). Unitary models based on the K matrix have been discussed by L. B. Redei [Nuovo Cimento **11A**, 279 (1972); **12A**, 249 (1972)].

²R. L. Sugar, Phys. Rev. D (to be published).

³G. F. Chew and A. Pignotti, Phys. Rev. **176**, 2112 (1968). For related developments of this idea, see G. F. Chew and C. DeTar, *ibid.* **180**, 1577 (1969); G. F. Chew and W. R. Frazer, *ibid.* **181**, 1914 (1969).

⁴This assumption differs in detail from CP. However, since it greatly simplifies the algebra but does not change the counting argument that output poles grow like N^2 , it seems justified to make this assumption.

⁵The reader may well wonder whether there is any justification for doing the sum over N in Eq. (47) by first summing over $N-r$ and then over r . The best justification at this point is that the resulting S matrix is unitary, since every matrix element of S may be written as $\exp(ih_p e^{(\alpha_P-1)Y})$ times the corresponding matrix element of S^M , the S matrix calculated by including only α_M . Since S^M , when calculated using the

Gaussian integral trick is unitary, so is S . For further justification see Eq. (62).

⁶If $h_p(B)$ were foolishly chosen as

$$h_p(B) = \hbar \exp[-\frac{1}{2}(B/R)^{1/2}],$$

then $\sigma_{\text{tot}} = \text{const} \times (Y^4)$, which violates the Froissart bound. This is an illustration of the fact that there are two essential ingredients in the proof of the Froissart bound: The first is unitarity, which the present model clearly satisfies. The second is analyticity in the Lehmann-Martin ellipse, which implies that the partial-wave amplitudes f_l fall off like $\exp(-al/\sqrt{s})$ for large l . [A. Martin, Phys. Rev. **129**, 1432 (1963)]. Thus in B space the amplitude [which is proportional to $(1-S)$] must fall off like $\exp(-aB)$. Since $h_p(B)$ is not determined by the model, but is rather an input to the model, the model in some sense does not have correct analyticity properties.

⁷This may seem bizarre, and it probably is, but it should be remembered that α_M is an *input* parameter, not necessarily related to the experimentally determined effective meson trajectory.

⁸This is suggested by the absorptive model: See, e.g., K. Gottfried and J. D. Jackson, Nuovo Cimento **34**, 735 (1964).

⁹This provides a simple but not very instructive proof of Eq. (49).

¹⁰See, for example, P. R. Halmos, *Finite Dimensional Vector Spaces* (Van Nostrand, New Jersey, 1958), p. 181. Halmos actually has a slightly different version of this principle, but a proof almost identical to his suffices to prove the version given here.